Non-Gaussian probability distribution of a velocity field in uniform straining-flow turbulence

M. Takaoka
Department of Mechanical Engineering, Faculty of Engineering Science, Osaka University, Toyonaka, Osaka 560, Japan
(Received 21 February 1995)

The non-Gaussian probability distribution of a velocity field *itself* is found in the numerical simulation of uniform straining flow turbulence. The distribution does not decrease as fast as a Gaussian distribution. The moment method to determine a limiting probability distribution, proposed by Sinai and Yakhot [Phys. Rev. Lett. **63**, 1962 (1989)] for the passive scalar field, is examined in detail for the present velocity field. It is found by the examination of the conditional probability distribution on vorticity magnitudes that the non-Gaussianity is caused in the tubelike high vorticity region, two-dimensional structure, appearing in the turbulent flow. The results are also compared with those of a passive scalar field and a three-dimensional flow with *two-dimensional structure*, which makes the contribution from pressure term to such distribution more apparent. It follows that the non-Gaussian distribution is due to the superior dissipation effect to the pressure (nonlinear) effect.

PACS number(s): 47.27.Gs, 47.27.Jv

I. INTRODUCTION

Probability distribution functions have been eagerly investigated in relation to the intermittency of fully developed turbulence. Intermittency may be noticed as the probability distribution is much flatter than the Gaussian for the large value of the variable. Intermittency of fully developed turbulence remains one of the most poorly understood phenomena. It is a generally accepted perception that homogeneous isotropic turbulence is approximately described by Kolmogorov's cascade theory [2], i.e., generation of small eddies by the process of breakup of the largest eddies. Landau [3] pointed out that the fluctuation of the dissipation rate in the field should be reflected, which leads to the modification of the original cascade theory.

The study of intermittency originates from the deviation of higher moments of velocity difference, i.e., structure functions, from the scaling law of the Kolmogorov theory, which should be modified to include the fluctuation of energy dissipation. Restricting ourselves to this point only, we should study two-point correlation functions instead of single-point ones. Many researchers have focused their attention on the non-Gaussian distribution of velocity derivatives, limiting the case of velocity differences. I think this non-Gaussianity is caused by the existence of intense vortex structure in turbulent flow. On the other hand, some theoretical models are based on the Gaussianity of velocity field, which is supported experimentally in isotropic turbulence. However, to the best of my knowledge, there is no theory to prove the Gaussianity of velocity field. I think it is not unusual that if the existence of a vortex structure causes a velocity derivative field to be non-Gaussian, it also affects the distribution of the velocity field itself. In this paper, I do not treat the original problem of turbulence intermittency but rather the role of vorticity structure in the distribution of velocity. Although this is just a preparatory study, I may give some insight into the original problem and improve upon some theoretical models.

Various laboratory and computer studies of isotropic turbulence show that the distribution of velocity is nearly Gaussian, while the distributions of velocity differences, vorticity, and passive scalars are non-Gaussian [4,5], whose foot decreases more gradually than the Gaussian, i.e., a flattened distribution. This flattened distribution becomes more pronounced as the Reynolds number increases, which suggests that any theory based on the Gaussianity of the field might be deficient for the sufficiently large Reynolds number or especially for the high-order moments of the velocity differences. Several models [1,6–10] have been proposed to explain this deviation from the Gaussian distribution.

Recent computer simulations reveal that there exist small-scale vortex structures produced by the competition between viscous relaxation and vortex stretching [11–13]. Most of these high vorticity regions appear as tubelike structures. These structures are thought of as the key to understand the intermittency of turbulence. Moreover, since this field may dominate the dynamics, it is important to investigate the possible effects of the relatively large-scale, long-living structures on small-scale properties of turbulence.

Most of the research about the intermittency has treated only the isotropic field. Little is known about the effects of anisotropy on the statistics, the distribution of velocity, its difference, and so on. Linear-flow turbulence, shear-, rotating-, and straining-flow turbulence have been investigated as a prototype of distortion and anisotropic turbulence. (A straining flow is sometimes referred to as a stagnation flow.) The rapid distortion approximation [14] is one of the well known theories for anisotropic turbulence. This approximation, however, is essentially linear, so that it predicts the normalized dis-

1063-651X/95/52(4)/3827(8)/$06.00

tribution will be *unchanged* under the rapid distortion. Although vortex stretching plays an important role to form the fine structure, it seems that straining-flow turbulence is less studied than shear- or rotating-flow turbulence. We, therefore, treat a straining-flow turbulence in the present study among the other linear flows.

The structure of this paper is as follows. The next section provides some notations and the basic equations with a uniform straining flow. Our purpose here is to clarify the effect, independent of external forces, of each term appearing in the Navier-Stokes equation on the non-Gaussianity. In Sec. III, we apply Sinai and Yakhot's method [1] to the present flow. Formally similar results are obtained for the velocity and passive scalar field except for the contribution from the pressure term. Numerical results about the probability distribution are shown in Sec. IV. We examine the method developed in Sec. III in detail and further investigate the numerical results by using the asymptotic method in Sec. V. Calculating the obtained expression numerically, we confirm that the imbalance between the pressure and viscous effect causes the non-Gaussian distribution. The results are discussed in the last section.

II. BASIC EQUATIONS WITH A UNIFORM STRAINING FLOW

We consider a viscous incompressible fluid with a uniform straining flow, a mean flow component. Let us divide the velocity field $\boldsymbol{v}$ into the mean and fluctuation components $\boldsymbol{u}$, as usual:

$$\boldsymbol{v} = (A_1x_1 + u_1, A_2x_2 + u_2, A_3x_3 + u_3). \tag{2.1}$$

Setting $A_1 + A_2 + A_3 = 0$, one knows $\mathrm{div}\boldsymbol{v} = \mathrm{div}\boldsymbol{u}$. And, for simplicity, all A_α's are set as time-independent constants in the present study.

In the following notation, repeated *latin* subscripts mean the summation from 1 to 3 while repeated *greek* subscripts mean no summation. Then, the governing equations for the fluctuation components of velocity field under the uniform straining flow are the Navier-Stokes equation and the continuity equation of the following form:

$$\frac{\partial u_\alpha}{\partial t} + A_jx_j\frac{\partial u_\alpha}{\partial x_j} + A_\alpha u_\alpha + u_j\frac{\partial u_\alpha}{\partial x_j} = -\frac{\partial p}{\partial x_\alpha} + \nu\frac{\partial^2 u_\alpha}{\partial {x_j}^2}, \tag{2.2}$$

$$\frac{\partial u_j}{\partial x_j} = 0, \tag{2.3}$$

where p and ν are, respectively, the fluctuation pressure and the kinematic viscosity, and the unperturbed pressure field is set $p_0 = A_j^2x_j^2/2$. The time evolution of a passive scalar field Θ, diffusing and passively advected by the velocity field, is determined by the equation

$$\frac{\partial \Theta}{\partial t} + A_jx_j\frac{\partial \Theta}{\partial x_j} + u_j\frac{\partial \Theta}{\partial x_j} = \kappa\frac{\partial^2 \Theta}{\partial {x_j}^2}, \tag{2.4}$$

where κ is the diffusivity.

Let us introduce a transformation [15]

$$X_\alpha = \exp(-A_\alpha t)x_\alpha \equiv T_\alpha x_\alpha, \tag{2.5}$$

which eliminates the explicit dependence on space variables, the second term on the left-hand side (LHS) of Eqs. (2.2) and (2.4). These basic equations are then rewritten, respectively, as

$$\partial_t u_\alpha + A_\alpha u_\alpha + u_jT_j\partial_j u_\alpha = -T_\alpha\partial_\alpha p + \nu T_j^2\partial_j^2 u_\alpha, \tag{2.6}$$

$$T_j\partial_j u_j = 0, \tag{2.7}$$

$$\partial_t\Theta + u_jT_j\partial_j\Theta = \kappa T_j^2\partial_j^2\Theta, \tag{2.8}$$

where $\partial_\alpha \equiv \frac{\partial}{\partial X_\alpha}$ and it is also used in the following notation. With a periodic boundary condition, one is able to use the standard pseudospectral method in the numerical simulation, although the coefficients are now a function of time.

III. MOMENT METHOD TO FIND PROBABILITY DISTRIBUTION

Sinai and Yakhot [1] investigated the limiting probability distribution of the passive scalar field by using the equation for passive scalar moments. They showed that if they chose the form of the conditional probability of a passive scalar field, $q(y|X)$ in their notation, and parameters in it, then their expression could fit the non-Gaussian probability distribution of the scalar obtained in the experiment. Parallel discussion to their idea is available also for the present problem. Let us introduce a normalized velocity,

$$v_\alpha^2 = \frac{u_\alpha^2}{\langle u_\alpha^2\rangle}, \quad (\langle v_\alpha^2\rangle \equiv 1). \tag{3.1}$$

The $\langle\,\rangle$ means the averaged quantity over the whole space. The governing equation for the $2n$th moments of the normalized velocity field is

$$\frac{\partial\langle v_\alpha^{2n}\rangle}{\partial t} = \frac{2n[\langle pT_\alpha\partial_\alpha u_\alpha\rangle - \nu\langle(T_j\partial_j u_\alpha)^2\rangle]}{\langle u_\alpha^2\rangle} \times\{(2n-1)\langle v_\alpha^{2n-2}w_\alpha^2\rangle - \langle v_\alpha^{2n}\rangle\}, \tag{3.2}$$

where

$$w_\alpha^2 = \frac{pT_\alpha\partial_\alpha u_\alpha - \nu(T_j\partial_j u_\alpha)^2}{\langle pT_\alpha\partial_\alpha u_\alpha\rangle - \nu\langle(T_j\partial_j u_\alpha)^2\rangle}. \tag{3.3}$$

The exact relation for the moments in the stationary state is

$$(2n-1)\langle v_\alpha^{2n-2}w_\alpha^2\rangle = \langle v_\alpha^{2n}\rangle. \tag{3.4}$$

Introducing the joint probability distribution $P(v_\alpha, w_\alpha)$, let us seek the solution satisfying the relations; $P(v_\alpha, w_\alpha) = P(v_\alpha)Q(w_\alpha|v_\alpha)$ and $v_\alpha^n P(v_\alpha)$ tends to zero for arbitrary n as v_α become infinity. Then, Eq. (3.4) can be read as

$$(2n-1)\int\int v_\alpha^{2n-2} w_\alpha^2 P(v_\alpha, w_\alpha) dv_\alpha dw_\alpha = \int\int v_\alpha^{2n} P(v_\alpha, w_\alpha) dv_\alpha dw_\alpha, \quad (3.5)$$

and partial integration about w_α further reduces it to

$$-\int v_\alpha^{2n-1}\left(\frac{dP(v_\alpha)}{dv_\alpha} q_\alpha(v_\alpha) + P(v_\alpha)\frac{dq_\alpha(v_\alpha)}{dv_\alpha}\right) dv_\alpha = \int v_\alpha^{2n} P(v_\alpha) dv_\alpha, \quad (3.6)$$

where use has been made of $q_\alpha(v_\alpha) = \int w_\alpha^2 Q(w_\alpha|v_\alpha) dw_\alpha$.

Then the differential equation for $P(v_\alpha)$ is

$$\frac{dP(v_\alpha)}{dv_\alpha} q_\alpha(v_\alpha) + P(v_\alpha)\frac{dq_\alpha(v_\alpha)}{dv_\alpha} = -v_\alpha P(v_\alpha). \quad (3.7)$$

And we can solve this equation as

$$P(v_\alpha) = \frac{C}{q_\alpha(v_\alpha)} \exp\left(-\int_0^{v_\alpha} \frac{x dx}{q_\alpha(x)}\right), \quad (3.8)$$

where C is a normalization constant.

The expression of (3.8) is similar to that obtained by Sinai and Yakhot, so the same arguments also hold here. If w_α is statistically independent of v_α, that is $q_\alpha(v_\alpha) \equiv 1$, we obtain the Gaussian distribution:

$$P(v_\alpha) = C \exp\left(-\frac{v_\alpha^2}{2}\right). \quad (3.9)$$

And if the distribution is non-Gaussian but close to it, we can expect the leading form to be $q_\alpha(v_\alpha) \approx c_0 + c_1 v_\alpha^2$ for a not too large value of $|v_\alpha|$ after considering the symmetry with $v_\alpha \leftrightarrow -v_\alpha$. And we also expect that $c_0 \approx 1$ and $|c_1|$ does not take as large a value. Then, Eq. (3.8) gives the explicit expression for the distribution as

$$P(v_\alpha) = \frac{C}{(c_0 + c_1 v_\alpha^2)^{1+\frac{1}{2c_1}}}. \quad (3.10)$$

In Fig. 1 are the lines of probability distribution for the several values of c_1. There, we set $c_0 = 1$, because by replacing the variables (v_α, C) with $(v_\alpha\sqrt{c_0}, Cc_0^{1+\frac{1}{2c_1}})$ we obtain the same figure. From this figure, one knows that the *positive* value of c_1 corresponds to the flattened distribution.

At this stage, the following two things should be noted. First, the contribution from the second term on the LHS of (2.2), the added term for the linear flow, disappears in the governing equation for the $2n$th moments of the normalized velocity field, Eq. (3.2), which also determines the probability distribution function of the velocity field. This corresponds to the fact that the rapid distortion approximation may not explain any deformation of a distribution function under the effect of a linear flow. In other words, under the linear transformation Gaussian distribution remains as it is. Second, considering the two variables (v_α, w_α) appeared in the joint probability distribution function, w_α is made of both its dissipation term and the pressure term, while for the passive scalar it is made of its diffusion term only [1]. Contemplating the reported fact that a velocity field is a Gaussian distribution and a passive scalar is not for the isotropic turbulence, one might think that the velocity (or passive scalar) field and its dissipation (or diffusion) field is not statistically independent, though the pressure field, through the nonlinear effect of mode coupling, causes the two fields (v_α and w_α) to be independent of each other.

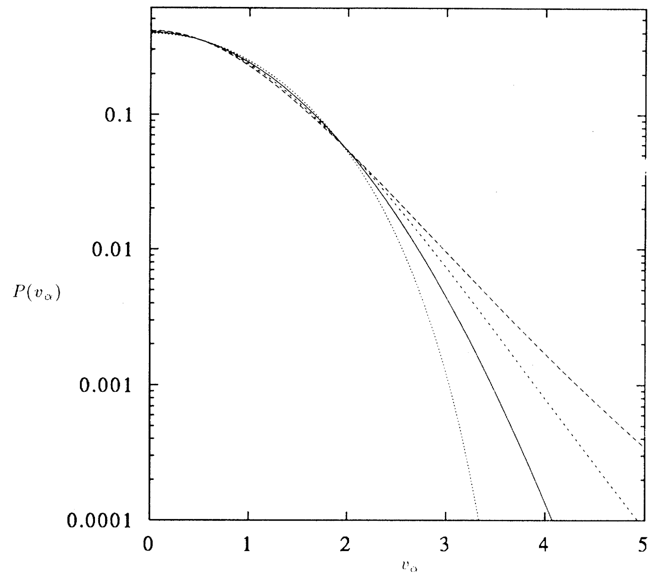

FIG. 1. Probability distribution of velocity when $q_\alpha(v_\alpha) = 1 - c_1 v_\alpha^2$. Solid line represents Gaussian distribution ($c_1 = 0$). Dotted, short-dashed, and long-dashed lines are, respectively, the lines for $c_1 = -1/16$, $1/16$, and $1/8$.

IV. NUMERICAL RESULTS FOR THE PROBABILITY DISTRIBUTION

In this section we present the numerical results obtained in the simulations of Eqs. (2.6) – (2.8). The initial field data (INI) were obtained by simulating the forced isotropic turbulence until the field achieved the statistically steady state. We simulate freely decaying turbulence for the isotropic case, all $A_\alpha = 0$, and the anisotropic case. Passive scalar fields are also simulated for both cases with the same initial condition as u_3 in INI. The parameters used in the present simulations are summarized in Table I. We will use shorthand notation, INI, FR6, ST4, YZ0, and YZ2, to represent each field for convenience. We chose $\nu = \kappa = 10/1024$, which guar-

TABLE I. Parameters used in the numerical simulation. N_i is the grid number in the ith direction.

Fields	$N_1 \times N_2 \times N_3$	(A_1, A_2, A_3)	$\langle \|\boldsymbol{u}\|^2/2 \rangle$	$\langle \|\boldsymbol{\omega}\|^2/2 \rangle$	$\langle \Theta^2 \rangle$	t_l	t_s	Re_λ
INI	128×128×128	(0,0,0)	1.312	57.25	0.441	2.347	0.093	32.58
FR6	128×128×128	(0,0,0)	0.761	35.74	0.190	2.179	0.118	23.84
ST4	256×128×128	(2, −1, −1)	1.176	59.27	0.254	2.032	0.092	28.51
YZ0	0×256×256	(0,0,0)	0.050	50.00		5.000	0.100	64.55
YZ2	0×256×256	(0,0,0)	0.018	13.94		6.378	0.189	43.57

antees the required numerical resolution as $K\eta = 2$ for $K = 64$ and $\langle |\boldsymbol{\omega}|^2 \rangle = 100$, where K is the maximum wave number and $\eta = (\nu^2/\langle |\boldsymbol{\omega}|^2 \rangle)^{1/4}$ is the Kolmogorov scale. Details of the numerical method and the results about the field structure will be shown in a separate paper [16]. Although several other types of ambient straining flows, such as $(A_1, A_2, A_3) = (+, +, -)$, are simulated, here we show only one typical case, $(A_1, A_2, A_3) = (+, -, -)$, which exhibits more clearly the (positive) straining effect on a probability distribution.

In Fig. 2, the $P(v_\alpha)$'s with the straining flow $(A_1, A_2, A_3) = (2, -1, -1)$ at time $t = 0.4$ (ST4) starting from INI are plotted to show how it deviates from Gaussian distribution by the straining (anisotropic) effect. This and the following graphs are made from *instantaneous* data, so that the points are scattered in the region where the variable takes a large value. We draw error bars to show positive-negative (left-right) asymmetry, which is zero ideally because of the symmetry of the system. Figure 2 clearly shows that the probability distribution in the positive straining direction, $P(v_1)$, is much flatter than the Gaussian distribution, which is similar to that observed in a passive scalar field. On the other hand, those in the other two directions are nearly Gaussian. For the lack of a sufficient data number, the plotted points for $P(v_2)$ and $P(v_3)$ begin to depart slightly for the region where the gradually decreasing foot is observed in $P(v_1)$, that is, $|v_\alpha| > 3$. But from this figure for ST4, one may safely say that the ambient uniform straining flow affects the distribution of velocity field. Although all distributions are converged into the Gaussian distribution in the region $|v_\alpha| < 3$, before being normalized the standard deviation in the positive straining direction is almost half of those in the other two directions.

To investigate the cause of this flattening and to know the relation with vortex structures, conditional probability distributions of v_1 on vorticity magnitudes are calculated and plotted in Fig. 3. The magnitude of vorticity norms are classified into five regions. One knows that the deviation from the Gaussian distribution is mostly made in the high vorticity region, $\omega_N\ (\equiv |\boldsymbol{\omega}|/\langle |\boldsymbol{\omega}|^2 \rangle^{1/2}) \geq 1$. Black marks are used in the figure to emphasize this phenomenon. These conditional probability distributions are not normalized to be 1 when integrated, but normalized to show the rate of the number of data, that is, summation for these five graphs gives 1.

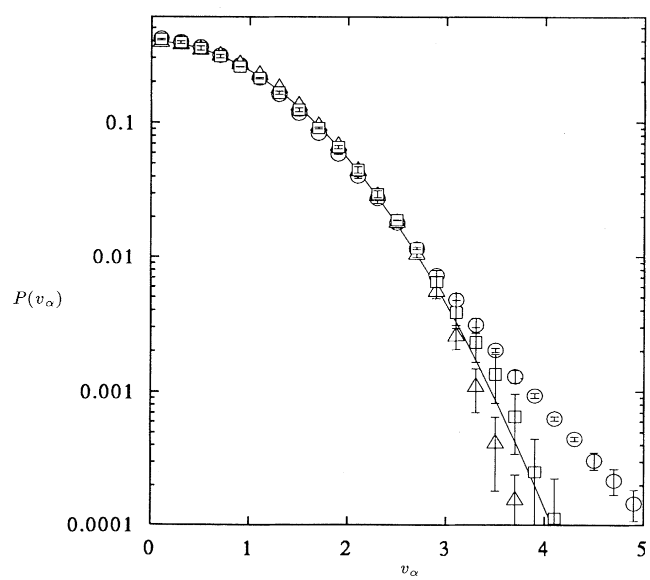

FIG. 2. Probability distribution of velocity for ST4. Circle, triangle, and square are, respectively, $P(v_1)$, $P(v_2)$, and $P(v_3)$. Error bars are also drawn to show the positive-negative asymmetry.

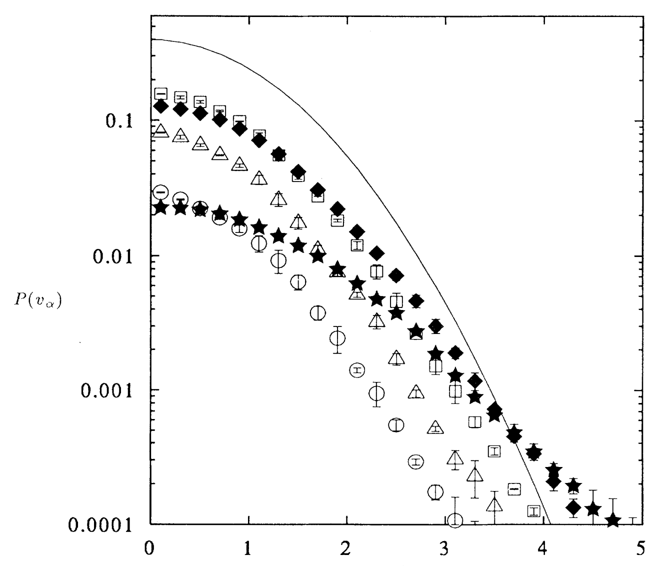

FIG. 3. Conditional probability distribution of the first component of velocity, v_1, on vorticity magnitudes for ST4. The magnitudes of vorticity norms are classified into five regions: ○, $0 \leq \omega_N < 1/4$; △, $1/4 \leq \omega_N < 1/2$; □, $1/2 \leq \omega_N < 1$; ◇, $1 \leq \omega_N < 2$; ⋆, $2 \leq \omega_N < 4$.

As pointed out in the preceding section, the formal difference appeared in the moment expression for passive scalar and vorticity is the contribution from the pressure term in the Navier-Stokes equation. To see the role of the nonlinear term, the pressure term, we also calculated the probability distribution of the passive scalar field in the freely decaying turbulence. In Fig. 4, the probability distribution of the passive scalar field without the straining flow is plotted with those of the velocity field for FR6, at $t = 0.6$ starting from INI. Because of the decrease in the Reynolds number and spending not enough time to evolve, the deviation of the passive scalar's distribution from Gaussian is not as large as that reported in the other larger Reynolds number simulation [4] and experiment [5]. We may be able to say that $P(v_\alpha)$ is still nearly Gaussian but $P(\theta)$ has a slightly larger foot, where $\theta^2 \equiv \Theta^2/\langle\Theta^2\rangle$. One then might think that the pressure, nonlinear, effect contributes to form the Gaussian distribution the viscous effect contributes to flattened distribution.

The conditional probability distribution of the passive scalar field is also calculated and plotted in Fig. 5. The deviation from Gaussian distribution is mostly seen in the region of low vorticity magnitude, $|\boldsymbol{\omega}_N| < 1/2$, which makes a contrast with the result for the conditional probability of v_1 for ST4. This may be understood by considering the opposite effect of nonlinearity, i.e., stretching: in a vorticity equation the stretching intensifies the field, whereas in an equation of the gradient of a scalar field it rarefies the field. Intense vorticity region and intense passive scalar region are mutually exclusive.

To confirm the effect of the pressure term and the vortex structures, we further simulated the *three-dimensional flow* having *two-dimensional structure*, that is, we retain only the Fourier elements with $k_x = 0$. The initial condition (YZ0) is random and different from the

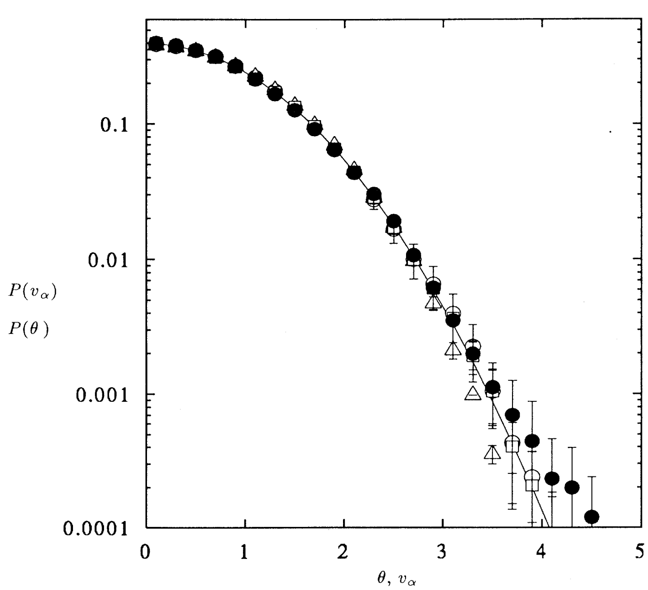

FIG. 4. Probability distribution of passive scalar (•) and velocity (○, △, □) for FR6.

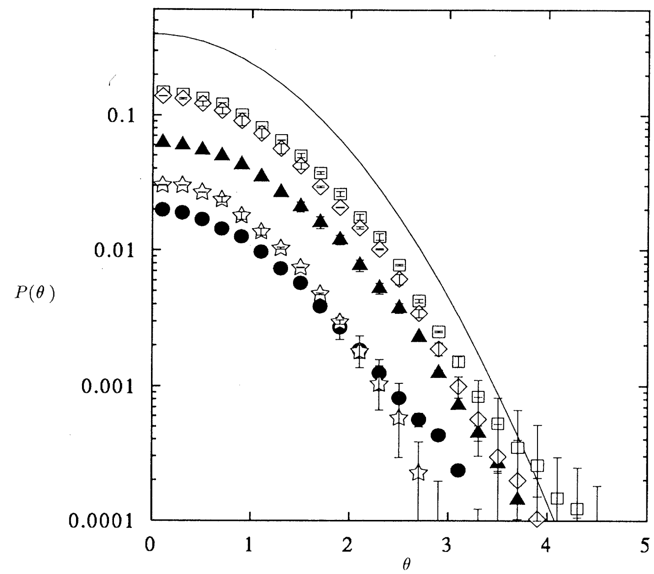

FIG. 5. Conditional probability distribution of passive scalar field on vorticity magnitudes for FR6. Usage of each mark is the same as in Fig. 3.

above simulations, INI. The initial energy spectrum has the form $E(k) \propto k^4 \exp(-k^2/k_0^2)$, where $k^2 = k_y^2 + k_z^2$, and $k_0 = 20$ and $\nu = 0.02$ are employed in the present simulation. It should be noted that there still remains three-dimensional aspects, vortex stretching and nonzero helicity, both of which are absent in a *usual* two-dimensional flow. The $P(v_\alpha)$'s are plotted in Fig. 6 for YZ2, at $t = 2$ starting from YZ0. The probability distribution of v_1 is deviated from Gaussian similar to that of the passive scalar field, while those of the other two

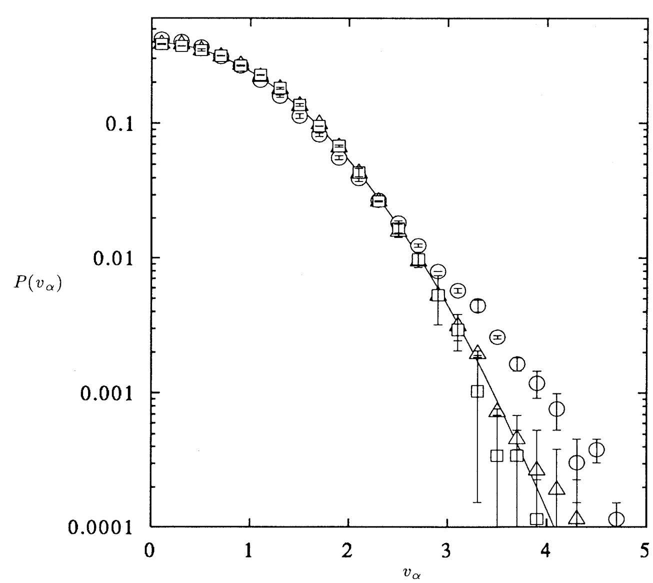

FIG. 6. Probability distribution of velocity field with the two-dimensional structure for YZ2. Circle, triangle, and square are, respectively, $P(v_1)$, $P(v_2)$, and $P(v_3)$.

TABLE II. The dependence of q_α on v_α, and q_s on θ.

Moment \ $\lvert v_\alpha \rvert$	$0-\frac{1}{2}$	$\frac{1}{2}-1$	$1-\frac{3}{2}$	$\frac{3}{2}-2$	$2-\frac{5}{2}$	$\frac{5}{2}-3$	$3-\frac{7}{2}$	$\frac{7}{2}-4$	$4-\frac{9}{2}$	$\frac{9}{2}-5$
					INI					
q_1	0.969	0.982	1.004	1.004	1.030	1.100	1.142	1.146	1.161	1.180
q_2	0.981	0.981	0.992	1.003	1.010	1.032	1.076	1.121	1.141	1.165
q_3	0.961	0.978	1.010	1.050	1.074	1.110	1.082	1.093	1.121	1.164
					ST4					
q_1	0.924	0.960	1.010	1.041	1.096	1.168	1.260	1.319	1.362	1.370
q_2	1.014	0.996	0.951	0.951	0.955	0.997	1.034	1.083	1.110	1.072
q_3	0.949	0.987	1.020	1.044	1.077	1.115	1.154	1.145	1.148	1.171
					FR6					
q_s	0.997	0.991	0.957	1.018	1.141	1.301	0.754	0.162	0.076	0.018
					ST4					
q_s	0.949	1.015	0.847	1.118	1.343	1.414	0.803	0.239	0.108	0.025

components, v_2 and v_3, are nearly Gaussian. This deviation is the most noticeable among the graphs exhibiting flattening and spreads over almost the whole range of v_α in Fig. 6. One can intuitively understand it by considering that the governing equation for v_1 begins to have the same form as that of a passive scalar field in two dimensions, advected by the "velocity" (v_2, v_3) and diffusing. The conditional probability distribution is also calculated. It shows that this flattening is mostly caused in the region where the vorticity has a large value, although the graphs are omitted here.

V. ASYMPTOTIC METHOD FOR THE NON-GAUSSIAN DISTRIBUTION

In order to check the argument in Sec. III to derive the probability distribution by using the relation between the moments, we calculate $q_\alpha(v_\alpha)$ for both fields whose probability distributions are nearly Gaussian and non-Gaussian obtained in the above simulations. The results are summarized in Table II. We divide v_α or θ into ten intervals, so that the fluctuation of the data is not small, perhaps because of the insufficient number of data. For the field INI, corresponding to the Gaussian distribution, all the values of the q_α's are nearly 1 as predicted in the moment method, but slightly increases with v_α. And consistent with the result that $P(v_1)$ shows flattened distribution and $P(v_2)$ and $P(v_3)$ are nearly Gaussian for ST4, q_1 is a clearly increasing function of v_1 while q_2 and q_3 are almost constant and equal to 1. Contrary to our expectation of the increase of q_s with θ, for both FR6 and ST4, q_s increases only in the range $\theta < 3$ and beyond this range it decreases rapidly. This might be due to the insufficient Reynolds number, which is supported by the fact that q_s for ST4 is larger than that for FR6.

The moment method, however, cannot explain why the $c_1 = \frac{1}{2}\frac{\partial^2 q_\alpha}{\partial {v_\alpha}^2}$ takes a *positive* value, even if a field with flattened distribution is isotropic. Furthermore, under the anisotropy of a linear flow, the rapid distortion approximation does not predict the deviation from Gaussian of a velocity field whose distribution is Gaussian before distortion. To the best of my knowledge, no theory can explain the non-Gaussianity of the velocity field in an anisotropic turbulence. We focus our attention here on the deviation from the isotropic turbulence under the effect of a uniform straining flow. Using the asymptotic method, we intend to explain the non-Gaussianity of the velocity field in the positive straining direction. Let us define the "one-directional dissipation rate":

$$\epsilon_\alpha = -T_\alpha p \partial_\alpha u_\alpha + \nu T_j^2 (\partial_j u_\alpha)^2, \tag{5.1}$$

the w_α^2 introduced in (3.3) is written as $w_\alpha^2 = \epsilon_\alpha / \langle \epsilon_\alpha \rangle$.

For $|A_\alpha t| \ll 1$, T_α may be expanded as $T_\alpha \approx 1 - A_\alpha t$, so that

$$\begin{aligned} \epsilon_\alpha &\approx -(1 - A_\alpha t) p \partial_\alpha u_\alpha + \nu (1 - A_j t)^2 (\partial_j u_\alpha)^2 \\ &\approx \{-p\partial_\alpha u_\alpha + \nu (\partial_j u_\alpha)^2\}(1 - A_\alpha t) \\ &\quad + (A_\alpha - 2A_j) t \nu (\partial_j u_\alpha)^2. \end{aligned} \tag{5.2}$$

On the other hand, we know the following three facts. First, the averaged quantity $\langle\,\rangle$ is independent of v_α^2. Second, when the field is homogeneous *isotropic* $(A_\alpha = 0)$ turbulence, the probability distribution of v_α is nearly Gaussian, which, in other words $\{-p\frac{\partial u_\alpha}{\partial x_\alpha} + \nu(\frac{\partial u_\alpha}{\partial x_j})^2\}$, is independent of v_α^2 in terms of the moment method. Third, rescaling the space variables, or the linear transformation (2.5), does not change the distribution. And if the original field $(A_\alpha t = 0)$ for the asymptotic expansion has the Gaussian distribution of velocity, we can expect that $\{-p\partial_\alpha u_\alpha + \nu(\partial_j u_\alpha)^2\}$ will continue to be independent of v_α^2.

Considering these three facts, one could say that the v_α^2 dependence of w_α^2 is that of $(\partial_j u_\alpha)^2$, so that our aim is reduced to knowing the v_α^2 dependence of $(\frac{\partial u_\alpha}{\partial x_j})^2$ for the *isotropic* $(A_\alpha t = 0)$ turbulence. When the flow field is isotropic and incompressible, then $\langle p\partial_\alpha u_\alpha \rangle = 0$, leading to the result $\langle \epsilon_\alpha \rangle > 0$. Then, the increase or decrease of w_α^2 with v_α^2, the sign of the second derivative (c_1), is the same as that of the last term on the right-hand side of Eq. (5.2). For convenience, if we assume $(A_1, A_2, A_3) = (2A, -A, -A)$, this term, $(A_\alpha - 2A_j)(\frac{\partial u_\alpha}{\partial x_j})^2$, can be read as

$$\alpha = 1, \quad 2A\left\{-\left(\frac{\partial u_1}{\partial x_1}\right)^2 + 2\left(\frac{\partial u_1}{\partial x_2}\right)^2 + 2\left(\frac{\partial u_1}{\partial x_3}\right)^2\right\}; \tag{5.3a}$$

$$\alpha = 2, \quad -A\left\{5\left(\frac{\partial u_2}{\partial x_1}\right)^2 - \left(\frac{\partial u_2}{\partial x_2}\right)^2 - \left(\frac{\partial u_2}{\partial x_3}\right)^2\right\}; \tag{5.3b}$$

$$\alpha = 3, \quad -A\left\{5\left(\frac{\partial u_3}{\partial x_1}\right)^2 - \left(\frac{\partial u_3}{\partial x_2}\right)^2 - \left(\frac{\partial u_3}{\partial x_3}\right)^2\right\}. \tag{5.3c}$$

In Table III are listed the numerical results of the v_α^2 dependence of $(\frac{\partial u_\alpha}{\partial x_\beta})^2$ for INI. It shows a clearly increasing property with $|v_\alpha|$ of the lateral derivative while those of the longitudinal derivatives are almost constant and equal to 1. The sign of the coefficient for the lateral derivative in Eq. (5.3a) is opposite those of Eqs. (5.3b) and (5.3c). If A is positive, ST4 is the case, the first one increases with $|v_\alpha|$ and the other two decrease. Following the above argument of the moment method, this is consistent with our numerical result of the probability distribution for ST4; see also Fig. 2. We might obtain the narrower distribution than the Gaussian for the velocity in the other two directions, if we could simulate a much larger Reynolds number flow.

VI. SUMMARY AND DISCUSSION

We have simulated the turbulent field with the uniform straining flow focusing our attention on the probability distribution. The non-Gaussian distribution of the velocity field, which is similar to those obtained for the passive scalar and velocity derivative fields in previous research [4,5], is found in the present anisotropic flow. The probability distribution of the velocity in the *positive* straining direction shows gradual decrease in its foot, while those in the other (contracting) directions are nearly Gaussian.

We further examined the moment method, proposed by Sinai and Yakhot [1], by checking the relation between the probability distribution and the variation of $q_\alpha(v_\alpha)$. Comparing with the results for the passive scalar and the *three-dimensional flow* with *two-dimensional structure*, we know the pressure term is indispensable for the Gaussian distribution. In other words, the non-Gaussian distribution is due to the superior dissipation effect to the pressure (nonlinear) effect.

To see the role of the intense vortex tube appearing in the turbulent flow, we calculated the conditional probability distribution on vorticity magnitudes for both the velocity in the straining direction and the passive scalar. For the velocity field the deviation is caused in the high vorticity region, while for the passive scalar it is caused in the low vorticity region, although both of them show similar non-Gaussian distribution. This might be understood by considering the opposite role of straining in the governing equations for $\nabla \times \boldsymbol{u}$ and $\nabla\Theta$. One may say in general that the velocity field parallel to the vortex tubes shows a flattened distribution, since we know that the vorticity is intensified in the straining direction and most of the vorticity tubes are aligned in this direction,

The asymptotic method proposed in the preceding section shows how one can reduce the non-Gaussianity problem in an anisotropic flow to that of the *isotropic* flow and the deviation is caused from the imbalance between the pressure effect and the viscous effect. This method succeeds in explaining the non-Gaussianity of the velocity in the straining direction. And furthermore, it pre-

TABLE III. The dependence of q_α of $(\frac{\partial u_\alpha}{\partial x_\beta})^2$ on v_α for INI.

Moment \ $\lvert v_\alpha \rvert$	0 – $\frac{1}{2}$	$\frac{1}{2}$ – 1	1 – $\frac{3}{2}$	$\frac{3}{2}$ – 2	2 – $\frac{5}{2}$	$\frac{5}{2}$ – 3	3 – $\frac{7}{2}$	$\frac{7}{2}$ – 4	4 – $\frac{9}{2}$	$\frac{9}{2}$ – 5
$(\frac{\partial u_1}{\partial x_1})^2$	1.007	0.990	0.992	0.969	0.971	1.002	1.015	1.023	1.030	1.023
$(\frac{\partial u_2}{\partial x_2})^2$	1.028	0.995	0.971	0.953	0.927	0.937	0.948	0.968	0.974	0.996
$(\frac{\partial u_3}{\partial x_3})^2$	1.005	0.978	0.975	0.991	1.003	1.008	0.978	0.988	0.993	1.044
$(\frac{\partial u_1}{\partial x_2})^2$	0.965	0.986	1.014	1.005	1.032	1.101	1.164	1.151	1.173	1.167
$(\frac{\partial u_2}{\partial x_3})^2$	0.977	0.983	1.001	1.004	1.030	1.045	1.094	1.123	1.159	1.174
$(\frac{\partial u_3}{\partial x_1})^2$	0.964	0.981	1.006	1.042	1.063	1.097	1.072	1.090	1.095	1.141
$(\frac{\partial u_1}{\partial x_3})^2$	0.953	0.975	1.002	1.021	1.058	1.148	1.186	1.204	1.217	1.270
$(\frac{\partial u_2}{\partial x_1})^2$	0.964	0.973	0.994	1.023	1.028	1.063	1.169	1.188	1.199	1.231
$(\frac{\partial u_3}{\partial x_2})^2$	0.936	0.975	1.031	1.086	1.121	1.173	1.144	1.147	1.212	1.249

dicts that if one could simulate a much larger Reynolds number flow, one might obtain the narrower distribution for the velocity in a *contracting* direction. This idea is also applicable to those problems with more general linear flow, such as (time-dependent) shear and/or rotating flow. But the Gaussian distribution of velocity and non-Gaussianity of velocity derivatives in an *isotropic* flow still remains unanswered in this asymptotic method.

ACKNOWLEDGMENTS

Numerical computation has been done on a SX3 computer in the Osaka University Data Processing Center. This work was partially supported by a Grant-in-Aid for Scientific Research from the Ministry of Education, Science and Culture of Japan.

[1] Ya. G. Sinai, and V. Yakhot, Phys. Rev. Lett. **63**, 1962 (1989).
[2] A. N. Kolmogorov, C. R. Acad. Sci. USSR **30**, 301 (1941).
[3] L. Landau and M. Lifshitz, *Fluid Mechanics* (Pergamon, New York, 1983).
[4] Z. She, E. Jackson, and S. Orszag, Proc. R. Soc. London, Ser. A **434**, 101 (1991).
[5] J. Z. Warhaft, Phys. Rev. Lett. **67**, 3503 (1991).
[6] Z. She, Phys. Rev. Lett. **66**, 600 (1991).
[7] R. Kraichnan, Proc. R. Soc. London, Ser. A **434**, 65 (1991).
[8] Z. S. She and S. A. Orszag, Phys. Rev. Lett. **66**, 1701 (1991).
[9] R. Benzi, L. Biferale, G. Paladin, A. Vulpiani, and M. Vergassola, Phys. Rev. Lett. **67**, 2299 (1991).
[10] E. A. Novikov, Phys. Rev. A **46**, R6147 (1992).
[11] E. D. Siggia, J. Fluid Mech. **107**, 375 (1981).
[12] R. M. Kerr, J. Fluid Mech. **153**, 31 (1985).
[13] I. Hosokawa and K. Yamamoto, J. Phys. Soc. Jpn. **58**, 20 (1989).
[14] A. A. Townsend, J. Fluid Mech. **98**, 171 (1980).
[15] M. Takaoka, J. Phys. Soc. Jpn. **60**, 2602 (1991).
[16] M. Takaoka, Phys. Fluids (to be published).